University of Dayton

eCommons

Electro-Optics and Photonics Faculty Publications

Department of Electro-Optics and Photonics

7-1-2021

Optical switching performance of thermally oxidized vanadium dioxide with an integrated thin film heater

Andrew M. Sarangan
University of Dayton, asarangan1@udayton.edu

Gamini Ariyawansa
Air Force Research Laboratory

Ilya Vitebskiy
Air Force Research Laboratory

Igor Anisimov
Air Force Research Laboratory

Follow this and additional works at: https://ecommons.udayton.edu/eop_fac_pub

 Part of the Electromagnetics and Photonics Commons, Optics Commons, and the Other Physics Commons

eCommons Citation

Sarangan, Andrew M.; Ariyawansa, Gamini; Vitebskiy, Ilya; and Anisimov, Igor, "Optical switching performance of thermally oxidized vanadium dioxide with an integrated thin film heater" (2021). *Electro-Optics and Photonics Faculty Publications*. 126.
https://ecommons.udayton.edu/eop_fac_pub/126

This Article is brought to you for free and open access by the Department of Electro-Optics and Photonics at eCommons. It has been accepted for inclusion in Electro-Optics and Photonics Faculty Publications by an authorized administrator of eCommons. For more information, please contact mschlangen1@udayton.edu, ecommons@udayton.edu.

Research Article | Vol. 11, No. 7 / 1 July 2021 / Optical Materials Express 2348
Optical Materials EXPRESS

Optical switching performance of thermally oxidized vanadium dioxide with an integrated thin film heater

ANDREW SARANGAN,[1,*] GAMINI ARIYAWANSA,[2] ILYA VITEBSKIY,[2] AND IGOR ANISIMOV[2]

[1]Department of Electro-Optics and Photonics, University of Dayton, Dayton, OH 45469, USA
[2]Air Force Research Laboratory, Sensors Directorate, Wright-Patterson AFB, OH 45433, USA
[*]sarangan@udayton.edu

Abstract: Optical switching performance of vanadium dioxide produced by thermal oxidation of vanadium is presented in this paper. A 100nm thick vanadium was oxidized under controlled conditions in a quartz tube furnace to produce approximately 200nm thick VO_2. The substrate was appropriately coated on the front and back side to reduce reflection in the cold state, and an integrated thin film heater was fabricated to allow in-situ thermal cycling. Electrical measurements show a greater than three orders of magnitude change in resistivity during the phase transition. Optical measurements exhibit 70% transparency at 1500nm and about 15dB extinction across a wide spectral band between 1000nm and 3000nm. These results are used to show a huge optical bistability effect in VO_2-based devices.

© 2021 Optical Society of America under the terms of the OSA Open Access Publishing Agreement

1. Introduction

Vanadium dioxide (VO_2) is a phase change material (PCM) that undergoes a dramatic structural change near room temperature. At low temperatures, it exists in a monoclinic crystalline state and exhibits properties of a semiconductor with a relatively high resistivity. As the temperature is elevated above 68°C, it abruptly switches to a hexagonal crystalline state. This state exhibits properties similar to that of a metal, with a negative bandgap, low resistivity and negative dielectric constant. As the temperature is allowed to cool down, it reverts back to the monoclinic state, albeit at a slightly lower switching temperature due to its built-in hysteresis [1]. The difference in resistivity between the two states is typically 3-4 orders of magnitude, with large changes in its optical constants. This switching has been shown to be very fast, on the order of nanoseconds [2]. These properties have made VO_2 an ideal candidate for optical switching applications, including optical bistability (OB) devices for realizing all-optical switching and memories [3,4], and for optical limiters used in the protection of sensors from high intensity laser damage [5,6].

VO_2 is most typically deposited using reactive physical vapor deposition from a vanadium source on heated substrates [7–9]. The substrate is typically heated to temperatures in the range of 500°C. Heating to such high temperatures inside a PVD chamber has a number of associated challenges due to poor thermal contact, contamination and uniformity, which results in reproduceability and scalability problems. In an earlier paper, we demonstrated an alternate technique where metallic vanadium films were thermally oxidized in an oxidation furnace to produce VO_2 [10]. This allows batches of wafers to be oxidized simultaneously using an external radiative source for heating. Additionally, this method also allows pre-patterning the vanadium metal, which is much simpler than post-patterning and etching of VO_2.

In this paper, we examine the optical switching properties of VO_2 films produced by thermal oxidation. For this, we use a device configuration with an integrated heating element. Current is applied through the heater to induce the phase change, while simultaneously measuring both its

#430751 https://doi.org/10.1364/OME.430751
Journal © 2021 Received 10 May 2021; revised 9 Jun 2021; accepted 9 Jun 2021; published 28 Jun 2021

Optical Materials EXPRESS

temperature and the optical transmission and reflection. The measured data is used in examining the switching properties such as extinction and optical bistability. We report the first experimental demonstration of temperature-induced optical switching on thermally oxidized vanadium dioxide films. Based on our measurements, a huge bistability effects in the case of all-optical switching have been predicted.

2. Thermal oxidation of vanadium

Vanadium metal films were deposited on cleaned double-side polished 2-inch diameter c-cut sapphire substrates using electron-beam thermal evaporation. The thickness of the film was 100nm. Due to the high reactivity of vanadium, a base pressure of $<10^{-6}$ Torr was achieved, with minimal time delay between unloading the wafers from the PVD chamber and the subsequent oxidation process. The metal-coated substrates were then loaded into a quartz tube furnace for oxidation. The pressure in the tube was maintained at 2.5mT using a turbomolecular pump and an oxygen flow controlled by a bleed valve. The temperature of the furnace was ramped up at a rate of 10°C/min, and held at 485°C for 6-hours, and then allowed to cool down. These conditions were previously determined to be the most optimum for oxidizing 100nm of vanadium into VO_2.

Oxidation will increase the thickness of the film depending on the density and molecular weight of the resulting oxide. Since these values are known for the various oxides of vanadium, the expected thickness change can be precisely calculated. Table 1 shows the volume change fraction for the most common oxides of vanadium.

Table 1. Common oxides of vanadium, their densities and weights, and the expected volume change when oxidized.

	Density g/cc	Molecular Weight g/mol	Volume Change
V	5.8	50.94	1
VO	5.76	66.94	1.32
V_2O_3	4.87	149.9	1.75
VO_2	4.57	82.94	2.05
V_2O_5	3.36	181.9	3.08

Based on the values listed in Table 1, we expect a thickness change of 2.05 when vanadium is oxidized to VO_2. Step-height measurements using a surface profiler were performed on all of our films before and after oxidation, and the ratio was found to be in the range between 1.9 and 2.1 confirming that the composition was dominantly VO_2. Other compositions have significantly different values, so variations in compositions, or mixed compositions, can be easily detected. This method of verifying composition through thickness measurement is an additional benefit of the thermal oxidation method. Our thermally oxidized VO_2 has also been previously studied using XPS, XRD and ellipsometry [10]. While it is theoretically possible for certain mixtures of V_2O_3 and V_2O_5 to produce a ratio close to that of VO_2 (specifically 77% V_2O_3 and 23% V_2O_5), neither V_2O_3 nor V_2O_5 exhibit a phase transition at 68°C. Since our films exhibited a very strong phase transition at 68°C, the volume expansion factor simply substantiated the conclusion that our film was dominantly VO_2.

3. Electrical testing

Sheet resistance measurements were done on all the samples using a four-point probe on a temperature controlled substrate stage. The results are plotted in Fig. 1. It shows a phase transition temperature of 68°C, with a 3-4 orders of magnitude of resistivity change. This resistivity contrast is among some of the highest reported in the literature, and validates the efficacy of producing VO_2 by thermal oxidation. Additionally, as the temperature was repeatedly cycled

Optical Materials EXPRESS

between 40°C and 90°C, both the hot-state and the cold state showed a clear but slow increase in resistivity. For the hot state, the resistivity increased from 2.02 mΩ·cm to about 3.6 mΩ·cm after 10 cycles. The cold state resistivity increased from 129Ω·cm to 200Ω·cm. Beyond 10 cycles there was no noticeable change in the resistvity. This behavior, which has also been reported by other authors, has been attributed to a change in oxygen concentration as well as an increase in micro fractures in the film [11,12].

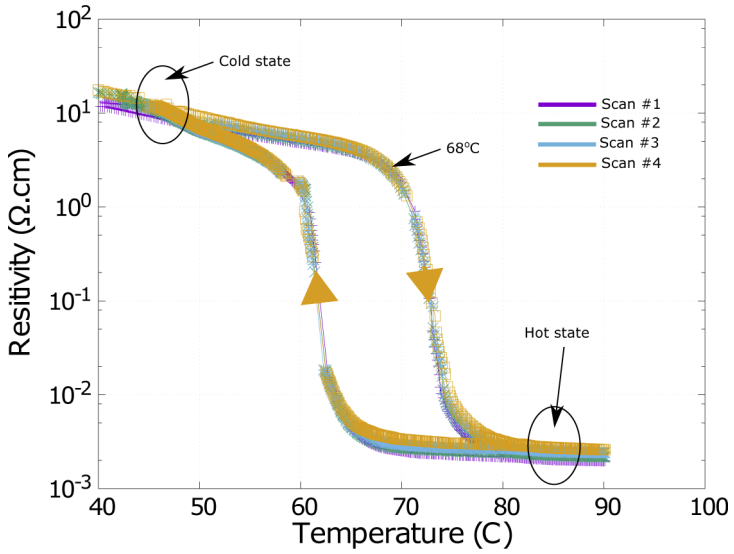

Fig. 1. Resisivity vs temperature scans of the thermally oxidized VO_2 showing a slow increase in resistivity with cycling.

4. Integrated heater and optical coating design

In order to perform optical testing, an integrated heater was designed and fabricated on the backside of the sapphire substrate. This consisted of a 400nm thick copper trace with a clear aperture at the center to allow the optical signal to pass through as shown in Fig. 2. The measured end-to-end resistance of the heater was about 10 Ω. A fine-wire thermocouple was attached near the central aperture to allow direct measurement of the temperature as a function of the heater current. With ambient cooling, the temperature rise as a function of heater power was calibrated to be about 25°C/W. Our objective here is to study the VO_2 as a function of temperature rather than examine the thermal constants of the system. Clearly, the thermal resistance value of 25°C/W would be highly dependent on the the ambient temperature as well as air flow and convection etc.

Two separate optical coatings were applied to this device to improve the optical transmission - one on the backside of the sapphire substrate, and one on the front side of the VO_2 film. The backside coating is very straightforward, because a simple quarter-wave film of index $\sqrt{n_s}$ can be used where n_s is the substrate index. Assuming $n_s = 1.74$ (sapphire), at a reference wavelength of 1500nm, the required film should have a refractive index of 1.32. MgF_2 was selected for this, whose refractive index is about 1.37 at 1500nm.

The front side coating requires a more detailed design because of the VO_2 film already present on the substrate. We can use the refractive index values for VO_2 that has been reported previously [13]. At a wavelength of 1500nm, the cold state index is $2.7 - j0.55$, and becomes $1.45 - j2.05$ in the hot state. These values can be used to design the top coating required for reducing the reflection. We can use the effective reflectance index method to design the layer structure. This principle is based on computing a lumped effective index that represents the multilayer structure

Optical Materials EXPRESS

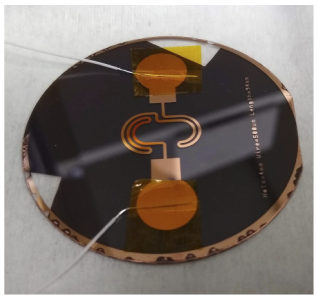

Fig. 2. VO_2 on a 2-inch sapphire wafer with an integrated thin film heating element.

for the purposes of calculating reflection. The details of this method are described elsewhere [14,15]. The effective reflectance index contour of the solution is shown in Fig. 3. The contour starts at the refractive index of sapphire at a reference wavelength of 1500nm (n_s = 1.74). VO_2 in the cold state is depicted by the solid purple line, and the green line shows the required film to bring the effective reflectance index to 1.0 (hence eliminating reflection). This film has a refractive index of 1.78 and a thickness of 160nm. We can also examine what happens when the VO_2 switches to the hot state. Using the same index of 1.78 and the 160nm thickness, the end-point of the contour moves to $0.52 - j0.31$. Applying this value into the normal incidence Fresnel equation results in a value of 21%. Therefore, we can expect the refection to switch between a low reflective state and 21% as the VO_2 switches from cold to hot state. For this material, we used Al_2O_3, which has a refractive index of 1.73 at 1500nm. The overall layer structure of the fabricated device is shown in Fig. 4.

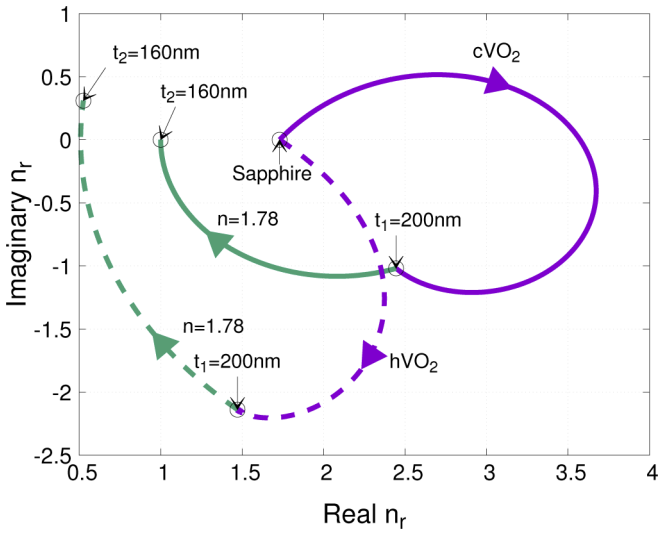

Fig. 3. Effective reflectance index contour of the single-layer antireflection design on top of the 200nm VO_2 film on sapphire.

Figure 5 shows the SEM cross sectional image of the top side of the substrate (VO_2 and Al_2O_3). The distinctive polycrystalline structure of the VO_2 is clearly evident from this figure. The crystal sizes are on the order of 200nm with distinctly visible crystal facets. Based on these images and the electrical and optical performance results, we believe this is among the highest quality VO_2 films reported in the literature, and compares favorably with other methods of synthesis [16,17].

Optical Materials EXPRESS

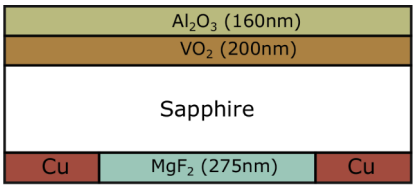

Fig. 4. Structure of the VO_2 device showing the layer structure.

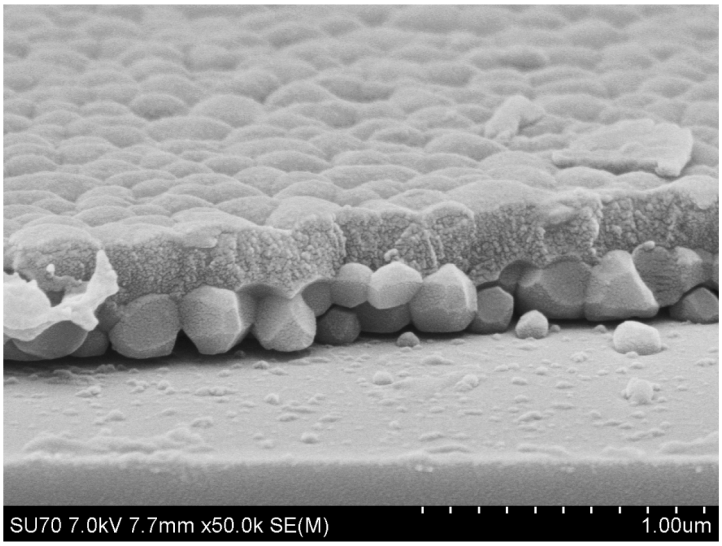

Fig. 5. SEM cross sectional image of the VO_2 polycrystalline layer with an Al_2O_3 layer above it.

5. Optical measurements

The completed device was mounted inside a Fourier Transform Infrared Spectroscopy (FTIR) system for transmission and reflection measurements. The current through the integrated heater was increased in discrete steps, and the temperature of the substrate was recorded using a fine-wire thermocouple bonded to the device near the central optical aperture. Since our design wavelength was 1500nm, the scan was taken between 1000nm and 3000nm wavelengths. The particle sizes seen in Fig. 5 are about five times smaller than the shortest measurement wavelength. Moreover, our film is absorptive. Therefore, we estimate the effects from scattering on the measurement to be minimal. Additionally, our FTIR system was optimized to minimize the impact of scattering through wide angle collection optics.

Figure 6 shows the measured transmission coefficient taken at different film temperatures. The peak transmission is 70% at a wavelength of 1800nm. Even though the antireflection was designed for 1500nm, the peak is red-shifted due to the intrinsic losses in the VO_2 film, which is higher at shorter wavelengths. As the film temperature rises above 70°C, we can see the transmission across the entire band abruptly drop to near zero.

Figure 7 shows the measured reflection spectra, taken at an incident angle of 10° from the normal. The reflection reaches a minimum at 1500nm in the cold state, which is consistent with the antireflection design. In the hot state it rises to 30%−50% across the band in the hot state. We can note that the reflection at 1500nm is higher than the design value by about 5% in the cold and hot states. This is primarily due to the single-layer anti-reflection films (Al_2O_3 and MgF_2) whose

Optical Materials EXPRESS

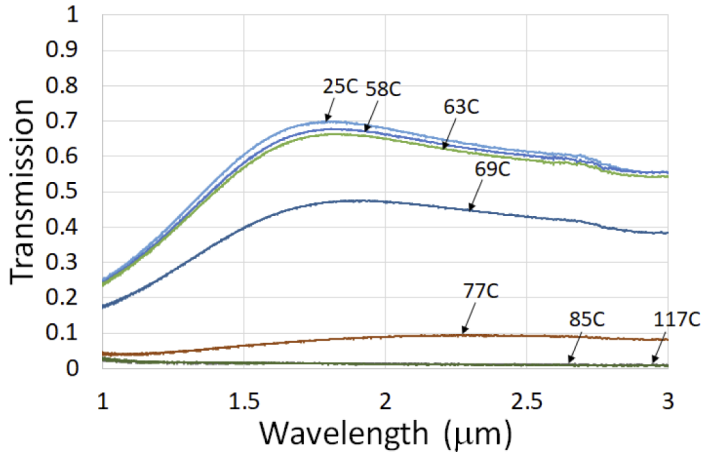

Fig. 6. Transmission spectra taken at increasing film temperatures using the integrated thin film heater.

refractive indices were not an exact match to the design values of 1.78 and 1.32. Additionally, we should note that our design goal was to maximize the transmission in the cold state and minimize the transmission in the hot state. The change in reflection is only incidental to this objective. It is possible, however, to design a different structure to maximize the reflection modulation.

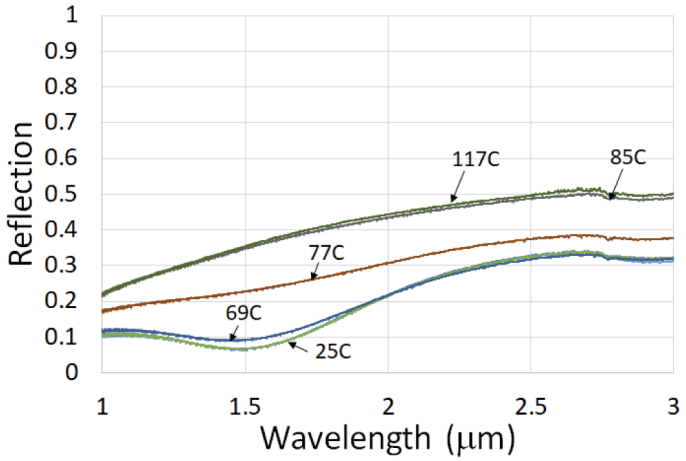

Fig. 7. Reflection spectra taken at increasing film temperatures using the integrated thin film heater.

Figure 8 shows the absorption calculated from the previous two plots using $1 - R - T$. In general, we can see that the absorption is lower at longer wavelengths. This is due to the declining loss-tangent values of VO_2 at longer wavelengths. The cold state has the lowest absorption, and rises to about 60%–70% in the hot state. We can also see that the absorption rises to a higher value during the phase transition, and then slightly declines as the transition is complete.

Figure 9 shows the calculated ratio between the hot state and cold state transmission coefficients, expressed in decibels. This extinction coefficient is often the most useful number in switching applications. We should note that the hot state transmission is very low (less than 1%) and the measurement is limited by the background noise. A more careful measurement with a smaller

Optical Materials EXPRESS

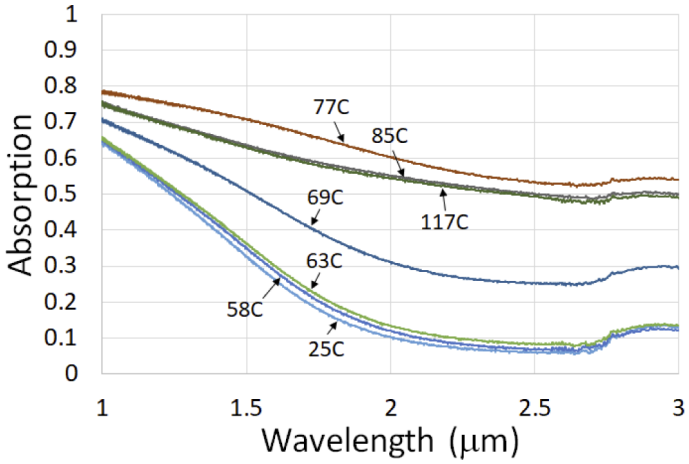

Fig. 8. Absorption spectra for increasing film temperatures.

background noise should yield a higher extinction. Nevertheless, the ratio is still in excess of 15dB, and is adequate for a large number of applications.

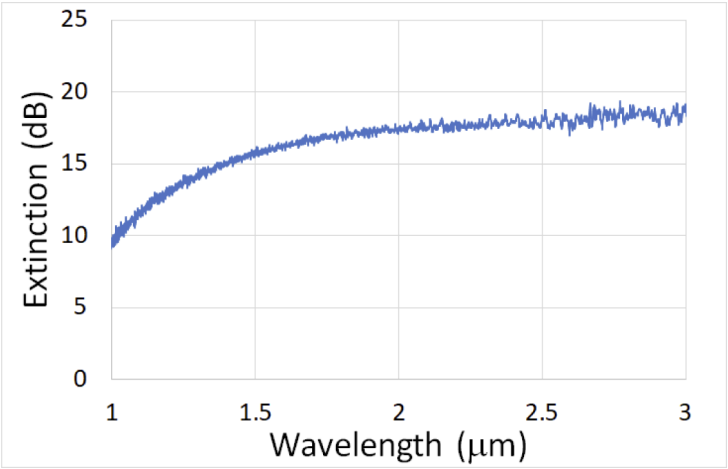

Fig. 9. Extinction coefficient calculated as the ratio between the cold and hot transmission coefficients.

Figures 10 and 11 show the absorption and transmission at three different wavelengths (1.5μm, 1.75μm and 2.0μm) as a function of film temperature during the heat-up and cool-down phases. The hysteresis seen here is consistent with the electrical hysteresis in Fig. 1. Again, we can see the momentary rise in absorption near the trailing edge of the phase transition, around 77°C.

Optical Materials EXPRESS

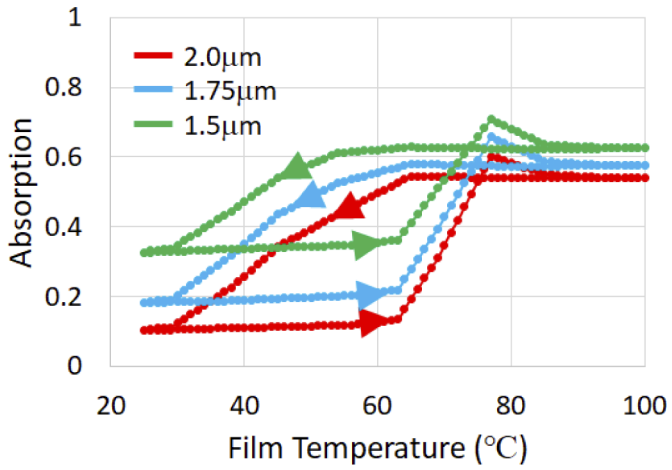

Fig. 10. Absorption at 1.5μm, 1.75μm and 2.0μm during the heat-up and cool-down cycles.

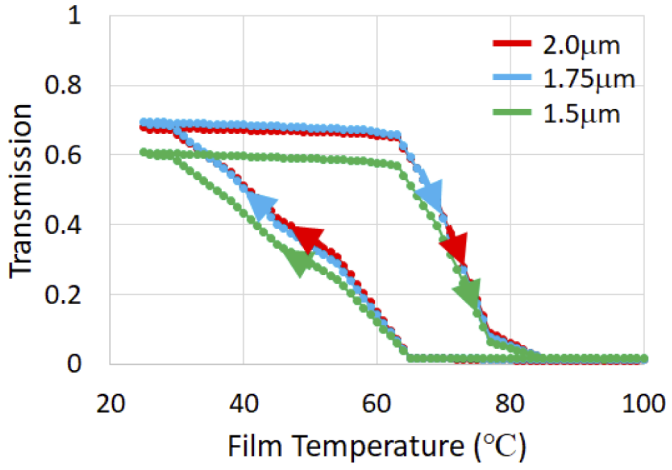

Fig. 11. Transmission coefficients at 1.5μm, 1.75μm and 2.0μm during the heat-up and cool-down cycles.

Optical Materials EXPRESS

6. Optical bistability

Although in this work we used electrical heating to induce the switching, the same effect can also be realized through optical absorption of an incident beam. Furthermore, if the relationship between absorption and incident intensity is nonlinear, this can lead to optical bistability. Optical bistability associated with the light-induced heating is somewhat similar to that associated with optical nonlinearity. In either case, for a given input light intensity, the system can have two or even more stable states. In the case of light-induced heating, the bistability can occur when the absorption is a growing function of the temperature (see, for example, [18] and references therein). In the particular case of heat-related phase transition, a huge optical bistability involving a run-away temperature effect can be expected if the absorption in the hot phase is significantly higher than that in the cold phase. According to Fig. 10, our system satisfies the above condition, except for the narrow trailing edge just above 77°C during the heating stage. To assess the effect of light-induced heating (instead of the electrical heating element), we can use the temperature dependence of absorbance given in Fig. 10 along with a simple Newton approximation for heat exchange. The relation between the input light intensity and the VO_2 film temperature can be written as

$$I_{in}\, A(T_f) = h(T_f - T_A) \tag{1}$$

where h (presumed constant) describes the thermal exchange with the ambience, I_{in} is the input intensity, T_f is the film temperature, T_A is the ambient temperature, and $A(T_f)$ is the experimentally measured absorbance presented in Fig. 10. The absorbance $A(T_f)$ is a hysteretic function of temperature. To obtain the VO_2 film temperature $T_f(I_{in})$ as a function of the input light intensity, we use Eq. (1) together with the experimentally measured absorbance $A(T_f)$. The result is shown in Fig. 12 for three separate wavelengths of 1.5μm, 1.75μm and 2.0μm. We see that the film temperature abruptly rises from 65°C to a much higher value due to the increase in absorption as a result of the phase transition of VO_2. This jump in temperature will be higher at longer wavelengths, and this can potentially result in a runaway temperature effect leading to a possible catastrophic failure of VO_2.

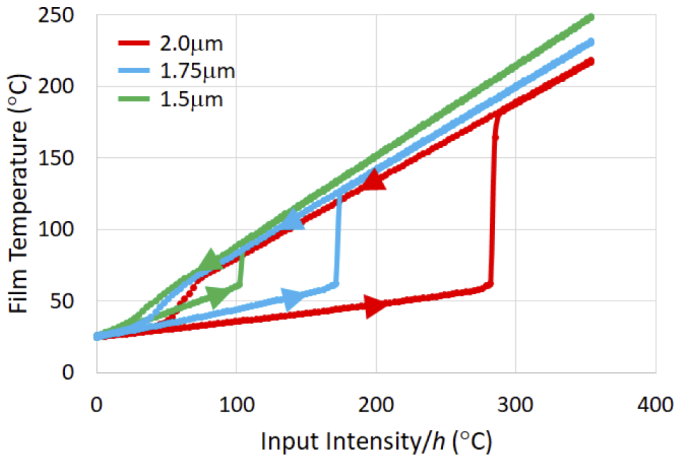

Fig. 12. Film temperature T_f vs I_{in}/h calculated using the measured absorption and transmission coefficients at 1.5μm, 1.75μm and 2.0μm wavelengths.

The computed transmitted intensity as a function of the input intensity is shown in Fig. 13 for 1.5μm, 1.75μm and 2.0μm wavelengths. We can see that the magnitude of the bistability (which is the range of input intensities for which there are two stable output values) is much larger at 2.0μm than at 1.5μm. This is due to the smaller difference in absorption between the cold and

Optical Materials EXPRESS

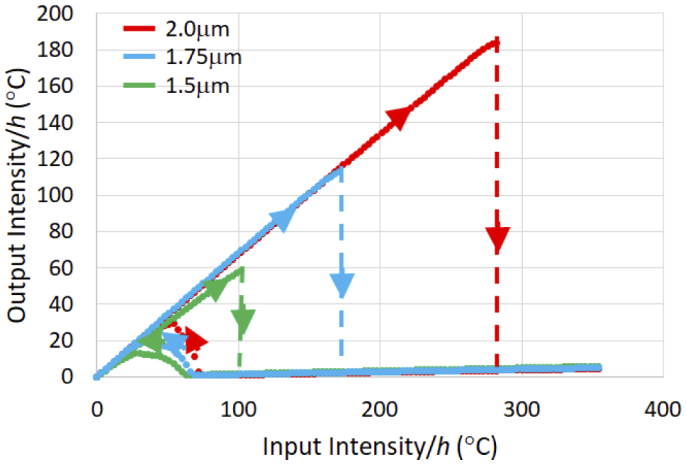

Fig. 13. Optical bistability calculated using the measured absorption and transmission coefficients at the wavelengths of 1.5μm, 1.75μm and 2.0μm.

hot states at 2.0μm compared to 1.5μm. In the case of an optical pulse, this will result in the leading edge and the trailing edge of the pulse switching at different intensity values.

Bistability has many important uses, such as optical memory, pulse shaping and optical logic circuits [3]. It is worth noting that, in VO_2, this bistability is unrelated to the hysteresis effect of VO_2. Even in the absence of any thermal hysteresis the difference in optical absorption between the cold and the hot state would be sufficient to cause this bistability. The presence of any addition thermal hysteresis will only help to enhance this bistability effect. This bistability can be computed using our measured results by considering the absorption and transmission as a function of film temperature.

7. Discussion and conclusions

We have demonstrated in this paper that high quality VO_2 films can be produced by thermally oxidizing a vanadium metal film. This process is significantly simpler and more scalable compared to the currently used reactive PVD or CVD processes. The polycrystalline grain sizes are on the same order of magnitude as the film thickness (200nm), which rival or exceed the quality of films produced using other methods. Sheet resistance measurements show a cold state resistivity of 100Ω-cm and a hot state resistivity of 3mΩ-cm, with a resistivity contrast of three orders of magnitude. Additionally, the stoichiometry of the resulting oxide can be inferred from film thickness measurements. Oxidation of V to VO_2 produces a thickness increase by a factor of 2.05. However, this work does not include a comparison of VO_2 produced using other methods. Literature reports contain significant range of performance values, and we do not feel a useful conclusion could be drawn from a quantitative comparison with other methods.

We were able to demonstrate a 70% transmission through a 200nm thick VO_2 film using an antireflection structure, and achieved a switching ratio of 15dB. This level of extinction is adequate for optical limiting applications. Although for demonstration purposes we have used an integrated thin film heater, it is also possible to use the incident light beam as the trigger that causes the phase transition. We show that this will result in a large optical bistability due to the difference in absorption between the hot and cold states, which is further enhanced by the built-in hysteresis of VO_2.

Funding. Air Force Office of Scientific Research (SFFP, LRIR 18RYCOR013).

Disclosures. The authors declare that there are no conflicts of interest related to this article.

Optical Materials EXPRESS

Data availability. Data underlying the results presented in this paper are not publicly available at this time but may be obtained from the authors upon reasonable request.

References

1. M. E. A. Warwick and R. Binions, "Advances in thermochromic vanadium dioxide films," J. Mater. Chem. A **2**(10), 3275–3292 (2014).
2. P. Markov, R. E. Marvel, H. J. Conley, K. J. Miller, R. F. Haglund, and S. M. Weiss, "Optically monitored electrical switching in VO_2," ACS Photonics **2**(8), 1175–1182 (2015).
3. H. M. Gibbs, *Optical Bistability: Controlling Light with Light* (Elsevier, 1985).
4. E. Abraham and S. D. Smith, "Optical bistability and related devices," Rep. Prog. Phys. **45**(8), 815–885 (1982).
5. O. B. Danilov, V. a. Klimov, O. P. Mikheeva, A. I. Sidorov, S. a. Tulskii, E. B. Shadrin, and I. L. Yachnev, "Optical limitation of Mid-IR radiation in vanadium dioxide films," Tech. Phys. **48**(1), 73–79 (2003).
6. W. Wang, Y. Luo, D. Zhang, and F. Luo, "Dynamic optical limiting experiments on vanadium dioxide and vanadium pentoxide thin films irradiated by a laser beam," Appl. Opt. **45**(14), 3378 (2006).
7. Y. Y. Luo, S. S. Pan, S. C. Xu, L. Zhong, H. Wang, and G. H. Li, "Influence of sputtering power on the phase transition performance of VO_2 thin films grown by magnetron sputtering," J. Alloys Compd. **664**, 626–631 (2016).
8. C. Ba, S. T. Bah, M. D'Auteuil, P. V. Ashrit, and R. Vallée, "Fabrication of high-quality VO_2 thin films by ion-assisted dual AC magnetron sputtering," ACS Appl. Mater. Interfaces **5**(23), 12520–12525 (2013).
9. M. Tangirala, K. Zhang, D. Nminibapiel, V. Pallem, C. Dussarrat, W. Cao, T. N. Adam, C. S. Johnson, H. E. Elsayed-Ali, and H. Baumgart, "Physical Analysis of VO 2 Films Grown by Atomic Layer Deposition and RF Magnetron Sputtering," ECS J. Solid State Sci. Technol. **3**(6), N89–N94 (2014).
10. P. Guo, Z. Biegler, T. Back, and A. Sarangan, "Vanadium dioxide phase change thin films produced by thermal oxidation of metallic vanadium," Thin Solid Films **707**, 138117 (2020).
11. N. A. Semenyuk, V. I. Surikov, Y. V. Kuznetsova, V. I. Surikov, and V. K. Volkova, "The effect of thermal cycling on the properties of $VO_2 \pm Y$ materials," J. Phys.: Conf. Ser. **1260**(6), 062022 (2019).
12. V. I. Surikov, V. I. Surikov, N. Semenyuk, O. Lyah, and Y. Kuznetsova, "Mechanical fracture of vanadium dioxide during thermal cycling," Procedia Eng. **152**, 711–714 (2016).
13. M. Currie, M. A. Mastro, and V. D. Wheeler, "Characterizing the tunable refractive index of vanadium dioxide," Opt. Mater. Express **7**(5), 1697 (2017).
14. A. Sarangan, "Design of metal-dielectric resonant-cavity thin-film structures using the effective reflectance index method," J. Opt. Soc. Am. B **35**(9), 2294 (2018).
15. A. Sarangan, *Optical Thin Film Design* (CRC Press, 2020).
16. S. Chen, J. Lai, J. Dai, H. Ma, H. Wang, and X. Yi, "Characterization of nanostructured VO_2 thin films grown by magnetron controlled sputtering deposition and post annealing method," Opt. Express **17**(26), 24153 (2009).
17. D. Hou, Y. Lu, and F. Song, "Effects of substrate temperature on properties of vanadium oxide thin films on Si substrate," in *Second International Conference on Photonics and Optical Engineering*, C. Zhang and A. Asundi, eds. (2017), p. 102560R.
18. A. Kuznetsov, "Optical bistability driven by a first order phase transition," Opt. Commun. **81**(1-2), 106–111 (1991).

131.238.109.28 {ts '2021-12-02 15:13:52'}